INTERNATIONAL JOURNAL FOR NUMERICAL METHODS IN ENGINEERING, VOL. 39, 3175–3194 (1996)

A GENERAL FORMULATION OF EQUILIBRIUM MACRO-ELEMENTS WITH CONTROL OF SPURIOUS KINEMATIC MODES: THE EXORCISM OF AN OLD CURSE

E. A. W. MAUNDER

School of Engineering, University of Exeter, U.K.

J. P. MOITINHO DE ALMEIDA AND A. C. A. RAMSAY

Department of Civil Engineering, IST, Technical University of Lisbon, Portugal

SUMMARY

This paper illustrates a method whereby a family of robust equilibrium elements can be formulated in a general manner. The effects of spurious kinematic modes, present to some extent in all primitive equilibrium elements, are eliminated by judicious assembly into macro-equilibrium elements. These macro-elements are formulated with sufficient generality so as to retain the polynomial degree of the stress field as a variable. Such a family of macro-elements is a new development, and results for polynomials of degree greater than two have not been seen before. The quality of results for macro-equilibrium elements with varying degrees of polynomial is demonstrated by numerical examples.

KEY WORDS: equilibrium elements; spurious kinematic modes; macro-elements

1. INTRODUCTION

The concepts of equilibrium elements and spurious kinematic modes are here introduced. Equilibrium elements offer possibilities of providing alternative solutions which give considerable scope for taking advantage of their results: e.g. dual analyses become possible which can provide bounds on quantities of interest such as the discretization errors, 'safe' designs of structures can be achieved when the lower bound theorem of plasticity is applicable. They have not however gained widespread popularity due to their relative complexity, the difficulties of incorporating into conventional software, and the more general problem with spurious kinematic modes.

The main tasks in formulating equilibrium elements are those of defining stress fields in elements, and assembling the elements. One approach[1-3] has been to utilize stress functions (such as Airy stress functions) interpolated from nodal values in a similar way to displacement fields. The principle of minimum complementary energy is then appropriate in formulating equations for a system of elements. However, the imposition of boundary conditions is not so straightforward. An alternative approach defines stress fields directly within elements (e.g. as polynomial functions), and also introduces 'secondary' quantities in the form of displacement connection variables associated with element boundaries.[1,2,4-6] Elements defined in this way are generally termed 'hybrid' elements. The displacement variables allow assembly to proceed, for example, with a stiffness method. Alternatively a force method is feasible[7,8] if dual force connection variables are defined.

CCC 0029–5981/96/183175–20 *Received 17 May 1995*

Displacement variables can be associated with displacements of discrete points, e.g. conventional nodes, or nodes associated only with the sides of elements, or modes of displacement of the sides of elements. A strong form of element interface equilibrium is not generally achieved when corner node displacements are included. This is due to the fact that the corresponding nodal forces are not directly associated with interfaces. However, diffusion of tractions and complete equilibrium may be locally enforced by using appropriate side displacement modes. The side displacement modes and internal stress fields defined for an element may give rise to spurious kinematic modes. These are modes of relative displacements of the sides of an element which can occur without the presence of side tractions. These spurious modes are also referred to as zero energy modes, and they produce an element stiffness matrix which is rank deficient. This situation is similar to that which can occur with conventional displacement elements due to the use of reduced integration. For example the 8-noded isoparametric serendipity element with 2×2 Gauss quadrature has the spurious kinematic mode in the form of an hourglass.[9] However, unlike the case with displacement elements where such modes rarely propagate through a finite element mesh, the spurious modes with equilibrium elements are more common and they are more likely to propagate.

The main challenge with equilibrium elements is to be able to achieve complete equilibrium without hindrance from spurious kinematic modes. Most elements based on polynomial fields are bedevilled by these modes! In this paper it is intended to present an approach based on decomposing each element into an assembly of primitive elements to form a macro-element. For the primitive elements the internal stress fields and the modes of side displacements are considered in polynomial forms. Using these stress fields complete equilibrium may be achieved with specified boundary tractions. The concept of macro-elements

(1) ensures that the effect of spurious kinematic modes can be eliminated from an arbitrary finite element mesh, and
(2) enables elements of any degree to be formulated in a simple and efficient way.

Whilst the basic idea of using macro-elements is not new,[1] the proposed approach is more general, and should allow for a rethinking on the usual concepts for the use of equilibrium elements.

2. FORMULATION OF A PRIMITIVE EQUILIBRIUM ELEMENT

The formulation summarized here is based on that presented in References 4 and 10. In each element the stress field is approximated by a linear combination of independent continuous functions which satisfy the equilibrium equations with zero body forces. A stress field $\boldsymbol{\sigma}$ is expressed as

$$\boldsymbol{\sigma} = \mathbf{S}\mathbf{s} \tag{1}$$

where the columns of $\mathbf{S}$ represent n_S independent stress fields, and the vector $\mathbf{s}$ contains n_S stress field parameters.

The boundary displacements of each element are approximated by a linear combination of independent functions. These functions describe the modes of displacement of each side i as a separate entity, so that compatibility of displacements of the different sides of an element is not an *a priori* assumption. The displacement field $\mathbf{u}_i$ for side i is expressed as

$$\mathbf{u}_i = \mathbf{V}_i \mathbf{v}_i \tag{2}$$

where the columns of $\mathbf{V}_i$ represent the independent modes of displacement of side i. The displacement $\mathbf{u}$ of an arbitrary point on a side of an element can then be expressed as

$$\mathbf{u} = \sum_i \mathbf{V}_i \mathbf{v}_i = \mathbf{V}\mathbf{v} \tag{3}$$

by extending the functions in $\mathbf{V}_i$ to cover all sides of an element. Thus $\mathbf{V}_i$ has zero value on side j when $j \neq i$. The columns of $\mathbf{V}$ now represent n_V independent displacement modes for all sides of an element.

The hybrid fields of internal stress and boundary displacement are used to impose weak integral forms of boundary equilibrium and internal compatibility. Equilibrium on the boundary of an element e is imposed by:

$$\left[\int_{\partial e} \mathbf{V}^{\mathrm{T}}\mathbf{N}\mathbf{S}\,ds\right]\{\mathbf{s}\} = [\mathbf{D}]\{\mathbf{s}\} = \{\mathbf{g}\} = \left\{\int_{\partial e} \mathbf{V}^{\mathrm{T}}\mathbf{t}\,ds\right\} \tag{4}$$

where the 2×3 transformation matrix $\mathbf{N}$ resolves stress at a boundary point into traction components, and $\mathbf{t}$ represents applied boundary tractions.

A weak integral form of compatibility within an element is imposed by

$$\left[\int_{\partial e} \mathbf{S}^{\mathrm{T}}\mathbf{N}^{\mathrm{T}}\mathbf{V}\,ds\right]\{\mathbf{v}\} = [\mathbf{D}^{\mathrm{T}}]\{\mathbf{v}\} = \{\boldsymbol{\delta}\} = \left[\int_e \mathbf{S}^{\mathrm{T}}\mathbf{f}\mathbf{S}\,de\right]\{\mathbf{s}\} = [\mathbf{F}]\{\mathbf{s}\} \tag{5}$$

where $\mathbf{f}$ represents the constitutive relations:

$$\mathbf{f}\boldsymbol{\sigma} = \boldsymbol{\varepsilon} \tag{6}$$

The vectors $\mathbf{g}$ and $\boldsymbol{\delta}$ represent generalized tractions and deformations corresponding to stress parameters $\mathbf{s}$ and displacement parameters $\mathbf{v}$ respectively. Equations (4) and (5) can be written together for the primitive element $\mathbf{e}$ as

$$\begin{bmatrix} -\mathbf{F}^e & \mathbf{D}^{e^{\mathrm{T}}} \\ \mathbf{D}^e & \mathbf{0} \end{bmatrix} \begin{Bmatrix} \mathbf{s}^e \\ \mathbf{v}^e \end{Bmatrix} = \begin{Bmatrix} \mathbf{0} \\ \mathbf{g}^e \end{Bmatrix} \tag{7}$$

where matrices $\mathbf{D}^e$ and $\mathbf{F}^e$ are defined in equations (4) and (5) respectively. $\mathbf{F}^e$ is termed the natural flexibility matrix, and the superscript e now identifies the element.

It should be emphasized that the weak form of equilibrium expressed by equation (4) may become a strong form of equilibrium for arbitrary applied boundary tractions $\mathbf{t}$ when in polynomial form of degree p. This may occur when the columns of $\mathbf{V}$ and $\mathbf{S}$ generate complete polynomial displacements and equilibrating stress fields respectively of degree $\geqslant p$.

3. SPURIOUS KINEMATIC MODES

The origins and the consequences of spurious kinematic modes for equilibrium elements are reviewed in this section. The effects of these modes, which originate at the level of a single primitive element, can be demonstrated by means of the generalized tractions and deformations $\mathbf{g}^e$ and $\boldsymbol{\delta}^e$ which are related to $\mathbf{s}^e$ and $\mathbf{v}^e$ by the contragradient transformations in equations (4) and (5). These transformations involve the $n_V \times n_S$ matrix $\mathbf{D}^e$. The work done by displacements $\mathbf{v}^e$ with tractions equilibrating with stresses $\mathbf{s}^e$ is thus given by

$$\mathbf{s}^{e^{\mathrm{T}}}\mathbf{D}^{e^{\mathrm{T}}}\mathbf{v}^e = \mathbf{g}^{e^{\mathrm{T}}}\mathbf{v}^e = \mathbf{s}^{e^{\mathrm{T}}}\boldsymbol{\delta}^e \tag{8}$$

Clearly for all displacements $\mathbf{v}_r^e$ conforming with the n_r rigid body modes of an element

$$\mathbf{D}^{e^T}\mathbf{v}_r^e = 0 \tag{9}$$

Although not strictly necessary, it is here assumed that all the rigid body modes for each side of an element are permitted within $\mathbf{v}^e$.

Spurious kinematic modes $\mathbf{v}_{skm}^e$ are defined as all other non trivial solutions to

$$\mathbf{D}^{e^T}\mathbf{v}_{skm}^e = \mathbf{0} \tag{10}$$

Displacements satisfying equations (9) and (10) form the null-space of $\mathbf{D}^{e^T}$, represented by the matrix $\mathbf{C}^e$ which has dimensions $n_V \times (n_V - \text{rank } \mathbf{D}^e)$ and satisfies

$$\mathbf{D}^{e^T}\mathbf{C}^e = \mathbf{0} \tag{11}$$

For these displacements no work is done with any of the internal stress fields. The number of independent spurious kinematic modes, n_{skm}, is thus given by

$$n_{skm} = (n_V - n_r - \text{rank}\,\mathbf{D}^e) \tag{12}$$

and a necessary, but not sufficient, condition for an element to be free of spurious kinematic modes is that

$$n_S \geqslant n_V - n_r \tag{13}$$

Boundary tractions $\mathbf{t}$ applied to an element are admissible only if

(a) they are in overall equilibrium, i.e. they do no work with the rigid body modes, and
(b) they do not excite any spurious kinematic mode, i.e. they do no work with any such mode.

$\mathbf{t}$ is represented by $\mathbf{g}^e$ as defined in equation (4). It follows that for $\mathbf{t}$ to be admissible, $\mathbf{g}^e$ must satisfy:

$$\begin{aligned} &\mathbf{g}^{e^T}\mathbf{v}^e = \mathbf{0} \quad \text{for all } \mathbf{v}^e \text{ such that } \mathbf{D}^{e^T}\mathbf{v}^e = \mathbf{0} \\ &\text{or } \mathbf{C}^{e^T}\mathbf{g}^e = \mathbf{0} \end{aligned} \tag{14}$$

It is now possible to stipulate the conditions for strong equilibrium on the boundary of an element: the applied traction must be admissible and in polynomial form of degree $\leqslant p$, where p is the degree of the element. The degree p refers to the degree of the polynomial approximations assumed within, and on the boundary of, the element. On the other hand, tractions are inadmissible if they do not satisfy the homogeneous equation (14), and hence they would excite spurious kinematic modes which in effect deny the means for load transmission.

By analogy with skeletal structures, spurious kinematic modes can be considered like 'mechanisms', and consequently they also act like 'releases' which prohibit the transmission of certain generalized forces or 'stress resultants'. These two aspects of spurious modes are illustrated in the case of a primitive triangular element with degree $p = 1$ in Figure 1. For this element, $n_S = 7$, $n_V = 12$ and $n_r = 3$. The rank of $\mathbf{D}^e = 7$, which implies the existence of two spurious kinematic modes.

A typical spurious mode is shown in Figure 1 with relative values of side displacement modes for an equilateral element. Two other similar modes exist by reason of cyclic symmetry, however only two of the three are independent. Admissible side loads must do no work with any of the spurious kinematic modes, hence the normal tractions shown, which are statically equivalent to three couples, are inadmissible. It should be noted that when the degree p is increased for the primitive, to a value of 5 say, then in this case $n_S = 33$, $n_V = 36$, $n_r = 3$, and hence $n_S = n_V - n_r$. Thus the necessary condition of equation (13) for no spurious kinematic modes is satisfied.

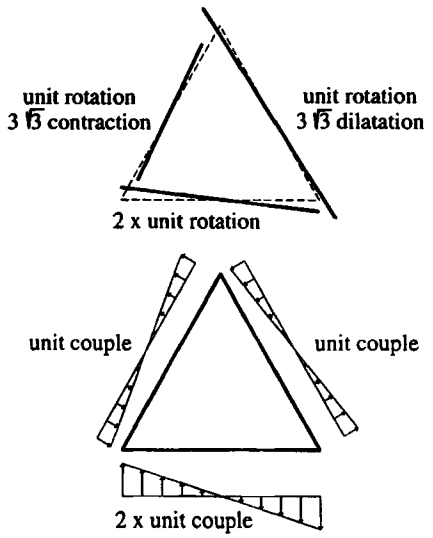

Figure 1. A typical spurious kinematic mode and an inadmissible load for an equilateral triangular primitive element with $p = 1$

However, it is found that $\mathbf{D}^e$ is rank deficient with a rank of only 30.[11] In this case, from equation (12), $n_{\mathrm{skm}} = 3$.

Although spurious kinematic modes originate at the element level, the main problem with such modes is that they may propagate throughout a finite element mesh, thereby leading to a rank deficient structural stiffness matrix for the system, and the possibility of load vectors being inadmissible. Such propagation is illustrated for patches of primitive triangular elements in Figure 2 for $p = 1$ and 2.

In each patch there exists just the one spurious kinematic mode for the system of elements. If these modes, or mechanisms, are excited by the applied loads, then a solution to the given problem is not feasible since the behaviour of the finite element model is described by an inconsistent system of equations. When mechanisms are not excited by the loads, the solution of the problem is unique in terms of stress distributions, but multiple in terms of displacements. This is indicated by a consistent, but singular, system of equations whose solution is not obtainable using solution algorithms designed for positive definite matrices.

As with the single element, the existence of spurious kinematic modes for an assembly of elements can be determined *a priori* to the formation of the stiffness equations, but this may involve significant computational effort. If $\mathbf{d}$ represents the modes of displacement of the sides or interfaces of an assembly of elements, the compatibility condition can be expressed by

$$\mathbf{A}\mathbf{d} = \mathbf{v} \tag{15}$$

where $\mathbf{v}$ now represents the side displacements of the set of all elements, and $\mathbf{A}$ is a Boolean type of assembly matrix. Let $\mathbf{D}$ now denote the block diagonal matrix:

$$\mathbf{D} = \begin{bmatrix} \mathbf{D}^1 & & \\ & \mathbf{D}^2 & \\ & & \ddots \end{bmatrix} \tag{16}$$

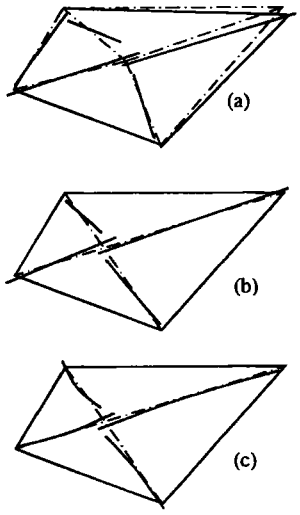

Figure 2. Spurious kinematic modes in a patch of primitive triangular elements: (a) $p = 1$, quadrilateral patch without diagonal subdivision; (b) $p = 1$, quadrilateral patch with diagonal subdivision; (c) $p = 2$, quadrilateral patch with diagonal subdivison

where $\mathbf{D}^e$ represents the matrix defined by equation (4) for element e. Then compatible spurious kinematic modes $\mathbf{d}_{skm}$ for the assembly must satisfy

$$[\mathbf{D}^T\mathbf{A}]\mathbf{d}_{skm} = \mathbf{0} \tag{17}$$

Thus the determination of these modes requires the computation of the rank and nullspace of $[\mathbf{D}^T\mathbf{A}]$.

4. A GENERAL APPROACH TO ANALYSIS WITH PRIMITIVE EQUILIBRIUM ELEMENTS

One possible way to treat the problems associated with spurious kinematic modes in a mesh has been proposed in References 4 and 10. A general formulation for equilibrium elements is presented there, and the possible spurious kinematic modes in a mesh are controlled by an equation solver which is capable of accounting for a matrix of reduced rank, but in a consistent system of equations.

As this solver encounters a dependent equation it zeroes the relevant variable, thus 'freezing' the spurious kinematic mode in an arbitrary position, and presents to the user a solution which is unique and of good quality in terms of the static variables, but whose quality may be doubtful in terms of kinematic variables. In cases where the system of equations is ill-conditioned, the definition by numerical techniques of those equations that are to be considered as dependent can be problematic. Also the *a priori* recognition of spurious kinematic modes and inadmissible loads for a mesh is not possible without significant additional analysis when this approach is used.

This approach allows for a very simple formulation of elements of any degree, but although the numerical problems associated with spurious kinematic modes may be controlled, the influence of these modes remains difficult to predict.

5. A ROBUST APPROACH BASED ON MACRO-ELEMENTS

Other authors have used assemblies of triangular equilibrium elements to form macro-elements, in such a way that the spurious kinematic modes are either totally eliminated, or remain internal to the macro-element. These macro-elements are either triangular or quadrilateral, as presented in Figure 3.

In the definition of macro-elements initially developed at Liége,[1,2,12-14] the position of the internal node P of the triangular macro-element is not constrained, and as was noted,[1] this macro-element is free of spurious kinematic modes. The position of P in the quadrilateral, however, was constrained to be positioned at the intersection of the diagonals. This macro-element was studied for polynomial approximations of the stress field up to the second degree and it was found that a single spurious mode was always present. This mode was explained with reference to a skeletal model formed from pin-jointed subtriangles. The stiffness matrix for the macro-element was formed by assembling the stiffness matrices of its four constituent elements, and then condensing out the internal degrees of freedom. However, some of these freedoms were indeterminate due to the spurious mode. The mode was blocked by the device of adding a fictitious bar which effectively coupled certain internal freedoms. The number of internal degrees of freedom to be eliminated was thus reduced by one. The stiffness matrix of the macro-element is correct as long as the spurious kinematic mode is not excited, and the fictitious bar remains unstressed. Figure 2(b) illustrates the important property of the spurious mode: it only involves relative displacements of the internal sides, and consequently all tractions applied to the external sides are admissible.

An alternative procedure[1,12,13] based on direct construction of stress fields was however found to be a more convenient way to obtain a stiffness matrix for a macro-element. By taking advantage of the oblique axes formed by the diagonals of the quadrilateral, statically admissible stress fields were formed directly so as to satisfy traction continuity between the elements. From these independent stress fields in the macro-element it is a straightforward matter to form a natural flexibility matrix and then a stiffness matrix. In the case of a hyperstatic element the principle of minimum complementary energy is invoked. The spurious kinematic mode thus does not explicitly appear in this procedure. More recently, other procedures based on directly satisfying internal traction continuity in triangular and quadrilateral macro-elements have been proposed.[15-18] Other authors have studied these macro elements in the context of elastic and elastoplastic analyses, and error estimation.[19-24]

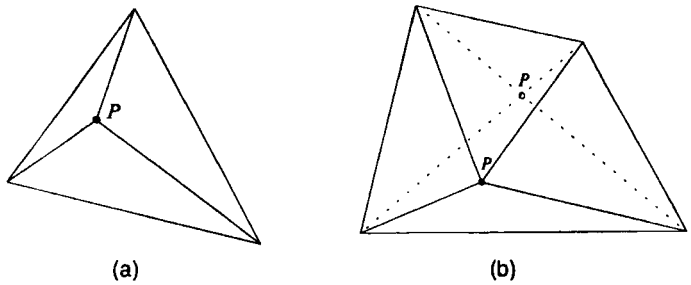

Figure 3. Macro-elements as assemblies of primitive elements: (a) triangular macro element; (b) quadrilateral macro element

The idea behind the macro-element is thus a simple one. For a macro-element to be effective, it should consist of an assembly of primitive elements for which any spurious kinematic modes which may exist only involve displacements of the internal sides, and consequently all tractions applied to the external sides are admissible. A mesh of such macro-elements will always be free of spurious mode problems provided the load is applied to the sides of the macro-elements. For the triangular macro-element there are no spurious kinematic modes irrespective of the degree of the stress field or the form of the internal geometry. In contrast, for the quadrilateral macro-element, the number and nature of the spurious kinematic modes are dependent on both the degree of the

Table I. Number and nature of spurious kinematic modes for a quadrilateral matcro-element

	Position of point P	
Degree of stress field	Intersection of diagonals	Arbitrary
$p = 1$	$n_{skm} = 1$ (benign)	$n_{skm} = 1$ (malignant)
$p \geqslant 2$	$n_{skm} = 1$ (benign)	$n_{skm} = 0$

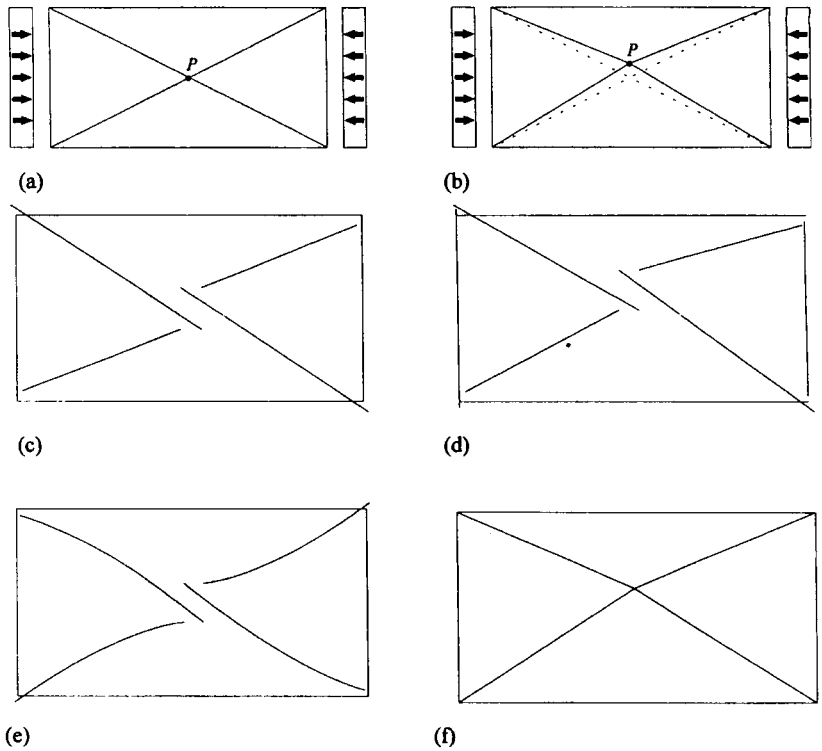

Figure 4. Displaced shapes for a single rectangular macro-element problem: (a) point P at intersection of diagonals; (b) Point P not at intersection of diagonals; (c) linear stress fields P at intersection; (d) linear stress fields P not at intersection; (e) quadratic stress fields P at intersection; (f) quadratic stress field P not at intersection

stress field and the form of the internal geometry. With reference to Figure 3, when P lies at the intersection of the diagonals, there is always one internal spurious kinematic mode for degree $p \geqslant 1$ (the 'benign' case). When P is in an arbitrary position and does not lie at the intersection of the diagonals, the kinematics depend on the degree p. In this case, when $p = 1$, there is one spurious kinematic mode, but now it involves relative movements of the external sides (the 'malignant' case). However when $p \geqslant 2$ there is no spurious kinematic mode. These properties of the quadrilateral macro-element are summarized in Table I, and illustrated in Figure 2, where the patches of primitive elements are now considered as macro-elements. *Thus for the more general case, the spurious mode is eliminated from the macro-element, and it is only in particular cases that the mode exists.* These findings are based on recent numerical studies reported by Maunder[18,25] and Ramsay,[11] and not on formal proofs. More comprehensive results and explanations for these findings are in preparation.

The different characteristics of the quadrilateral macro-elements when under load are illustrated in Figure 4. This figure illustrates the deformed shapes of four rectangular macro-elements when loaded with a uniform compressive stress, which is an admissible form of loading for all four elements. When spurious kinematic modes are present, their amplitudes, which are arbitrary, have been chosen so as to produce displacements of the same order of magnitude as for the other modes of displacement.

6. PROPOSED APPROACH

Based on the observations made in Sections 4 and 5, an efficient approach which combines generality with robustness is proposed. In this approach macro-elements are first defined as composed from primitive elements of general degree. Then the internal displacement variables are eliminated (condensed out) from the macro-element equations so as to obtain a stiffness matrix in terms of external variables. This approach requires that the composition of the macro-element either excludes spurious kinematic modes altogether, or if such modes are present they only involve the internal degrees of freedom. In the latter case the elimination procedure, as in Section 4, must recognize and account for dependent equations. The resulting stiffness matrix for the macro-element is then free of the singularities associated with spurious kinematic modes, and the assembly of all the macro-element matrices into a global set of equations follows the conventional procedure for a stiffness method.[9]

This approach is illustrated for the macro-element in Figure 5 composed of four primitive triangles. The triangles are numbered 1 to 4, the 'internal sides' or interfaces are numbered 1 to 4, and the external sides are numbered 5 to 8. Using the formulation presented in Reference 10, the

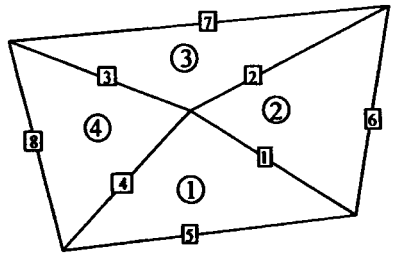

Figure 5. A general quadrilateral macro-element

governing system of equations for this assembly of primitive elements is

$$\left[\begin{array}{cccc|ccccc|ccccc}
-\mathbf{F}^1 & & & & \mathbf{D}_1^{1T} & & & \mathbf{D}_4^{1T} & & \mathbf{D}_5^{1T} & & & & \\
& -\mathbf{F}^2 & & & \mathbf{D}_1^{2T} & \mathbf{D}_2^{2T} & & & & & \mathbf{D}_6^{2T} & & & \\
& & -\mathbf{F}^3 & & & \mathbf{D}_2^{3T} & \mathbf{D}_3^{3T} & & & & & \mathbf{D}_7^{3T} & & \\
& & & -\mathbf{F}^4 & & & \mathbf{D}_3^{4T} & \mathbf{D}_4^{4T} & & & & & \mathbf{D}_8^{4T} & \\
\hline
\mathbf{D}_1^1 & \mathbf{D}_1^2 & & & & & & & & & & & & \\
& \mathbf{D}_2^2 & \mathbf{D}_2^3 & & & & & & & & & & & \\
& & \mathbf{D}_3^3 & \mathbf{D}_3^4 & & & & & & & & & & \\
\mathbf{D}_4^1 & & & \mathbf{D}_4^4 & & & & & & & & & & \\
\hline
\mathbf{D}_5^1 & & & & & & & & & & & & & \\
& \mathbf{D}_6^2 & & & & & & & & & & & & \\
& & \mathbf{D}_7^3 & & & & & & & & & & & \\
& & & \mathbf{D}_8^4 & & & & & & & & & &
\end{array}\right]
\left\{\begin{array}{c}
\mathbf{s}^1 \\ \mathbf{s}^2 \\ \mathbf{s}^3 \\ \mathbf{s}^4 \\ \mathbf{v}_1 \\ \mathbf{v}_2 \\ \mathbf{v}_3 \\ \mathbf{v}_4 \\ \mathbf{v}_5 \\ \mathbf{v}_6 \\ \mathbf{v}_7 \\ \mathbf{v}_8
\end{array}\right\} =
\left\{\begin{array}{c}
\mathbf{0} \\ \mathbf{0} \\ \mathbf{0} \\ \mathbf{0} \\ \mathbf{0} \\ \mathbf{0} \\ \mathbf{0} \\ \mathbf{0} \\ \mathbf{g}_5 \\ \mathbf{g}_6 \\ \mathbf{g}_7 \\ \mathbf{g}_8
\end{array}\right\}$$

where, for example, $\mathbf{D}_6^2$ refers to the submatrix of $\mathbf{D}^2$ concerning the displacement functions associated with side 6, and $\mathbf{v}_3$, $\mathbf{g}_5$ refer to displacements of and tractions on sides 3 and 5 respectively. This matrix equation can be written as

$$\left[\begin{array}{ccc}
-\mathbf{F} & \mathbf{D}_i^T & \mathbf{D}_e^T \\
\mathbf{D}_i & \mathbf{0} & \mathbf{0} \\
\mathbf{D}_e & \mathbf{0} & \mathbf{0}
\end{array}\right]
\left\{\begin{array}{c}
\mathbf{s} \\ \mathbf{v}_i \\ \mathbf{v}_e
\end{array}\right\} =
\left\{\begin{array}{c}
\mathbf{0} \\ \mathbf{0} \\ \mathbf{g}_e
\end{array}\right\}
\begin{array}{l}
\text{(compatibilty)} \\ \text{(internal equilibrium)} \\ \text{(external equilibrium)}
\end{array} \tag{18}$$

where subscripts i and e now refer collectively to the internal and external sides. As matrix $\mathbf{F}$ for the macro-element is positive definite, the first set of equations (18) expressing the compatibility conditions can be solved, taking advantage of the block structure of the matrices, to obtain

$$\mathbf{s} = \mathbf{F}^{-1}\mathbf{D}_i^T\mathbf{v}_i + \mathbf{F}^{-1}\mathbf{D}_e^T\mathbf{v}_e \tag{19}$$

This solution can be substituted in the second set of equations (18), which accounts for internal equilibrium:

$$\mathbf{K}_{ii}\mathbf{v}_i + \mathbf{K}_{ie}\mathbf{v}_e = \mathbf{0} \tag{20}$$

where $\mathbf{K}_{ii} = \mathbf{D}_i\mathbf{F}^{-1}\mathbf{D}_i^T$ and $\mathbf{K}_{ie} = \mathbf{D}_i\mathbf{F}^{-1}\mathbf{D}_e^T$.

Due to the possible presence of one spurious kinematic mode the solution for the $\mathbf{v}_i$'s from these equations may not be unique. Nevertheless, since these equations are always consistent, a solution can be obtained either by using an appropriate form of Gauss elimination, or by using the pseudo-inverse $\mathbf{K}_{ii}^+$ as determined by singular value decomposition.[26]

When $\mathbf{s}$ is replaced by $\mathbf{v}_e$ in the third set of equations (18), the macro-element stiffness matrix is obtained which transforms the external displacements to external tractions:

$$\bar{\mathbf{K}}\mathbf{v}_e = \mathbf{g}_e$$

where the general form of $\bar{\mathbf{K}}$ can be expressed as

$$\bar{\mathbf{K}} = [\mathbf{K}_{ee} - \mathbf{K}_{ie}^{\mathrm{T}}\mathbf{K}_{ii}^{+}\mathbf{K}_{ie}], \quad \text{where } \mathbf{K}_{ee} = \mathbf{D}_e\mathbf{F}^{-1}\mathbf{D}_e^{\mathrm{T}} \tag{21}$$

7. PROCESSING OF THE RESULTS

Once the global stiffness matrix is obtained the resulting system of equations can be solved using an algorithm appropriate for its structure: band, profile or sparse matrix.[9] The solution consists of the values of the displacement modes of the external sides of the macro-elements.

From these values the displacement modes of the internal sides of the macro-elements can be obtained from equation (20). However, these displacements should in general be disregarded when $\mathbf{K}_{ii}$ is singular, as then they only indicate one of the feasible solutions. Only the internal displacements, and not the stresses, are dependent on the spurious kinematic modes. The unique stress parameters are recovered from equation (19) after using equation (20):

$$\mathbf{s} = \mathbf{F}^{-1}[\mathbf{D}_e^{\mathrm{T}} - \mathbf{D}_i^{\mathrm{T}}\mathbf{K}_{ii}^{+}\mathbf{K}_{ie}]\mathbf{v}_e \tag{22}$$

8. NUMERICAL EXAMPLES

The behaviour and performance of the macro-elements discussed in this paper will be demonstrated through three numerical examples. In all the examples the macro-elements are rectangular, use diagonal subdivision, and the degrees of the stress fields are considered in the range 1 to 10. These properties of the macro-elements are chosen to simplify the examples, and are not constraints of the formulation. In Problem 1 equilibrium elements will be compared with conventional conforming displacement elements in order to compare the characteristics of the two different types of solution. Problem 2 illustrates the performance of equilibrium elements for a case with discontinuous material properties, whilst in Problem 3 a case involving a stress singularity due to geometry is investigated.

The stress plots that appear for the examples in the plates show unprocessed finite element stresses, i.e. no averaging or smoothing has been performed. For all the problems, the numbers of degrees of freedom (dof) tabulated for the equilibrium models refer to those associated with the displacements of the external sides of the macro-elements. Other measures of the dofs of the equilibrium models are possible which depend on considering the models as composed of primitive elements, rather than macro-elements, namely:

dof_d—the total number of displacement degrees of freedom;
dof_σ—the number of stress degrees of freedom.
dof_t—the total number of degrees of freedom (displacements and stresses) as used in Reference 10.

These quantities are compared in Table II for the meshes considered in Figure 6, when $p = 2$.

Problem 1. The geometry, boundary conditions and meshes are shown in Figure 6. The boundary tractions are linear and are defined to be in equilibrium with the stress field given in equation (23). It should be noted that whilst this stress field is statically admissible with zero body

forces, it is not kinematically admissible and is, therefore, invalid as the solution to the problem.

$$\sigma_x = x^2$$
$$\sigma_y = y^2 \tag{23}$$
$$\tau_{xy} = -2xy$$

Finite element analyses were performed using both conforming displacement elements (the standard 4-noded Lagrangian element and the 8-noded serendipity element) and the macro-equilibrium elements. Full integration was used in the analyses with both types of elements. The finite element strain energies U_h are shown in Table III and were calculated using Young's modulus $E = 210\,\mathrm{N/m^2}$, Poisson's ratio $\nu = 0{\cdot}3$, and a material thickness $t = 0{\cdot}1$ m with the

Table II. Degrees of freedom for the meshes in Figure 6 when $p = 2$

Mesh	dof (macro)	$\mathrm{dof_d}$	$\mathrm{dof_t}$	$\mathrm{dof_\sigma}$
1	72	168	360	192
2	240	624	1392	768
3	864	2400	5472	3072
4	3264	9408	21 696	12 288

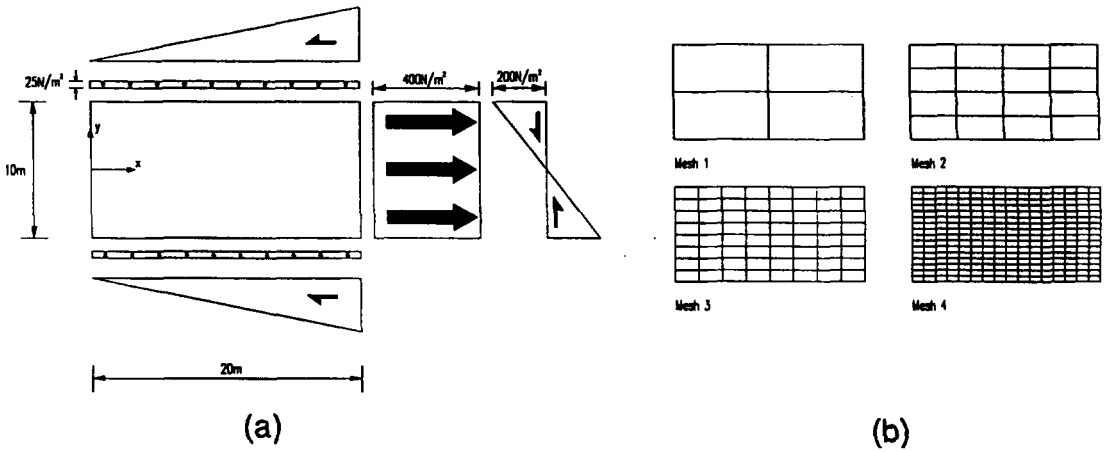

Figure 6. Problem 1: (a) the geometry and boundary conditions; (b) the meshes

Table III. Finite element results for Problem 1

	Conforming element				Equilibrium element			
Mesh	${}^4U_h^C$	dof	${}^8U_h^C$	dof	${}^1U_h^E$	dof	${}^2U_h^E$	dof
1	1702·598	18	2036·765	42	2050·422	48	2041·809	72
2	1953·359	50	2041·174	130	2042·310	160	2041·615	240
3	2019·156	162	2041·570	450	2041·655	576	2041·602	864
4	2035·951	578	2041·600	1666	2041·604	2176	2041·602	3264

assumption of plane stress. The right superscripts C and E refer, respectively, to the conforming and equilibrium models whilst the left superscripts refer to the number of nodes per conforming element, and to the degree of the stress field in the case of the equilibrium element.

The convergence of strain energies for the four types of element are shown in the graph of Figure 7. These results demonstrate the upper bounded nature of the strain energy for equilibrium models in contrast to the lower bound values achieved by conforming models. From the results given in Table III it is possible to state that the true value of the model strain energy U is such that $2041{\cdot}60015 \leqslant U \leqslant 2041{\cdot}60229$ (two additional decimal places are given).

The displaced shapes for Mesh 1 for the 4-noded displacement element and the linear equilibrium element are shown in Figure 8. The non-conforming edges of the equilibrium model are clearly seen.

Plate 1 demonstrates, qualitatively, the way in which equilibrium is violated when using conforming displacement elements. The discontinuities in the τ_{xy}-component of the stress across the element interfaces can be readily observed.

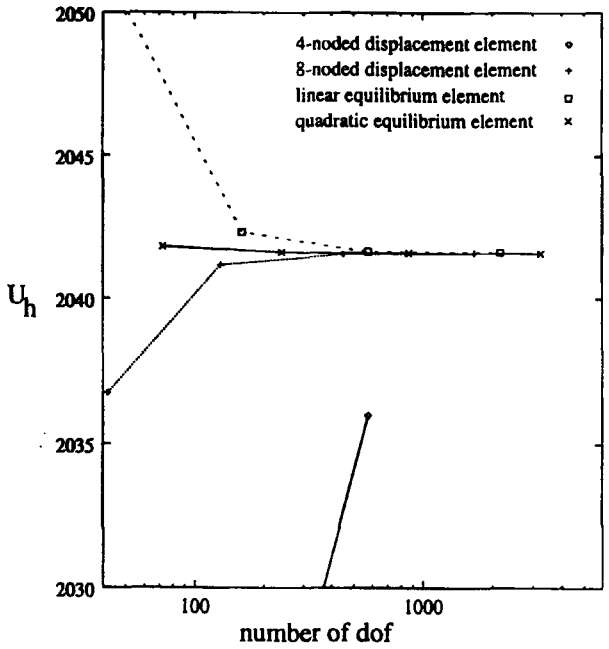

Figure 7. Convergence of strain energies for Problem 1

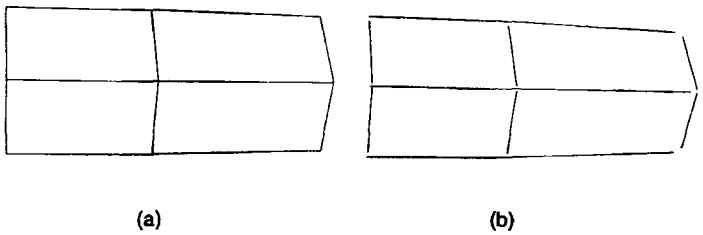

Figure 8. Displaced shapes for Mesh 1 of Problem 1: (a) conforming (4-noded) elements; (b) equilibrium (linear) elements

Problem 2. This problem compares the quality of results obtained by p and h refinement schemes with equilibrium elements. A rectangular membrane is formed from two square regions of different materials. Each material has a different Young's modulus but the same Poisson's ratio. The membrane is loaded with uniform tension as shown in Figure 9.

Region 1 has a Young's modulus of $E_1 = 100\,\mathrm{N/m^2}$ and for Region 2 $E_2 = 10\,\mathrm{N/m^2}$. Both regions have a Poisson's ratio of $\nu = 0{\cdot}3$ and a material thickness $t = 10\,\mathrm{m}$. An assumption of plane stress has been made for the purpose of this analysis. The coarsest mesh that can be used for this problem is the two element mesh shown as Mesh 1 in Figure 9(b). In addition to this mesh two uniform (h) refinements are also investigated (Meshes 2 and 3). In terms of p refinement, results for polynomial stress fields of degree one (linear) to degree five (quintic) are presented. The finite element strain energies U_h^E are shown in Table IV, and their convergence characteristics are shown graphically in Figure 10.

An idea of the different characteristics of the two types of refinement (p and h) can be obtained by studying the stress fields, and the distribution of normal traction along the material

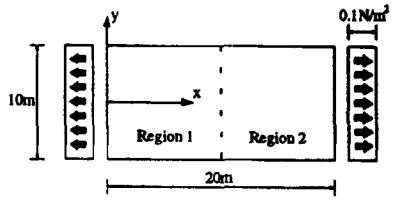

(a)

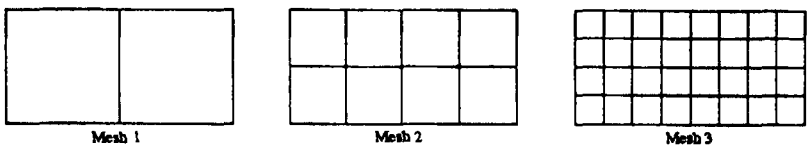

(b)

Figure 9. Problem 2: (a) the geometry and boundary conditions; (b) the meshes

Table IV. Finite element strain energy for Problem 2

	Mesh 1		Mesh 2		Mesh 3	
Degree (p)	U_h^E	dof	U_h^E	dof	U_h^E	dof
1	0·5477909	28	0·5467302	88	0·5462864	304
2	0·5464224	42	0·5462343	132	0·5461185	456
3	0·5463319	56	0·5461381	176	0·5460849	608
4	0·5461697	70	0·5461002	220	0·5460724	760
5	0·5461382	84	0·5460829	264	0·5460669	912

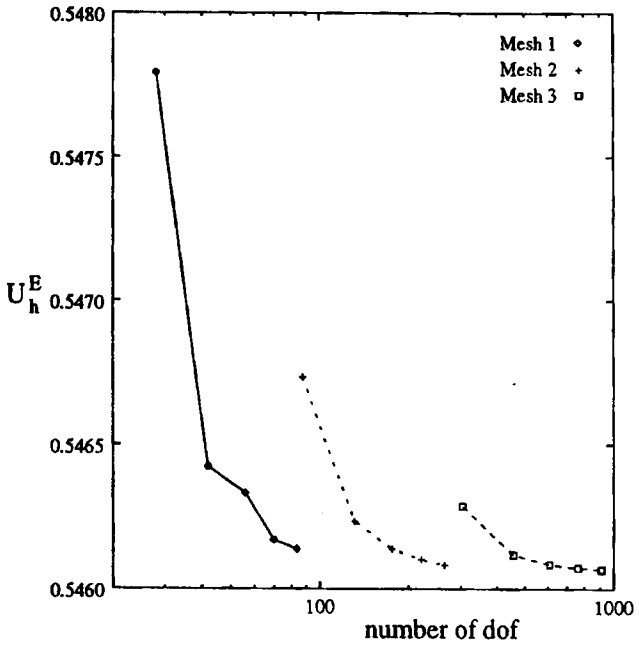

Figure 10. Convergence of strain energies for Problem 2

interface. For this purpose, contour plots of the σ_{xx}-component of stress are shown in Plate 2.

For Mesh 1 ($p = 1$) the discontinuities in stress that may occur across interfaces of equilibrium elements are clearly visible between the primitive elements. The discontinuities reveal the fact that each of the two square macro-elements is actually composed of four triangular primitive elements. Even though such stress discontinuities may occur, pointwise equilibrium across interfaces is strictly maintained. This is confirmed, for example, by the continuity in the x-direction of the σ_{xx}-component of stress at the interface between the two regions.

Figure 11 gives a more quantitative view of the stress distribution at the interface of the two regions by showing the σ_{xx}-component of stress plotted along this interface for a number of selected models. Discontinuities in the y-direction of the stress σ_{xx} are observed for Mesh 3 ($p = 1$), which violate the true solution, but do not violate equilibrium.

Problem 3. This problem involves a stress concentration due to a crack of infinitesimal width, and of length 5 m as shown for the symmetric half in Figure 12. The extent of the crack is illustrated by the thick line. The boundary tractions are evaluated from the following stress field which is both statically and kinematically admissible:[27]

$$\sigma_x = \frac{100}{\sqrt{r}} \cos\frac{\theta}{2}\left\{1 - \sin\frac{\theta}{2}\sin\frac{3\theta}{2}\right\}$$

$$\sigma_y = \frac{100}{\sqrt{r}} \cos\frac{\theta}{2}\left\{1 + \sin\frac{\theta}{2}\sin\frac{3\theta}{2}\right\} \tag{24}$$

$$\tau_{xy} = \frac{100}{\sqrt{r}} \sin\frac{\theta}{2}\cos\frac{\theta}{2}\cos\frac{3\theta}{2}$$

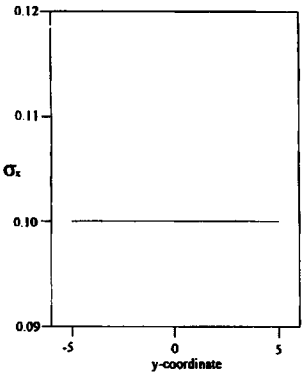

Mesh 1 (p=1)

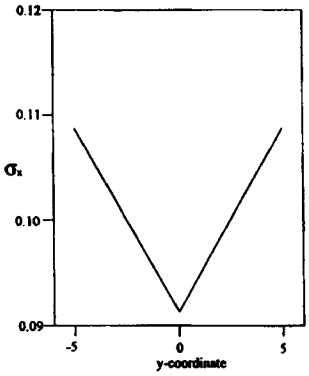

Mesh 2 (p=1)

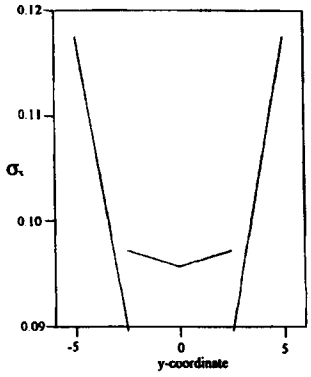

Mesh 3 (p=1)

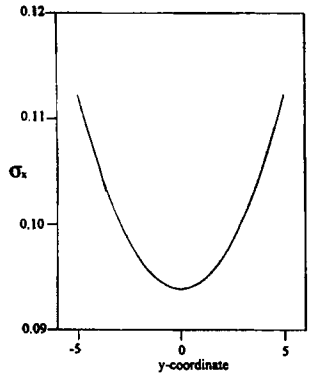

Mesh 1 (p=2)

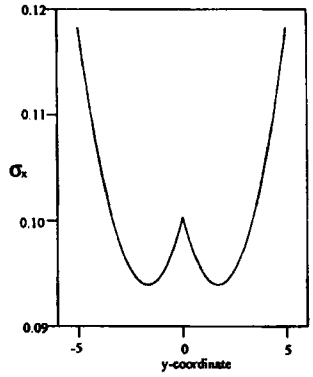

Mesh 2 (p=2)

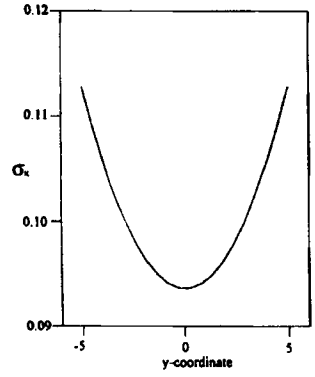

Mesh 1 (p=3)

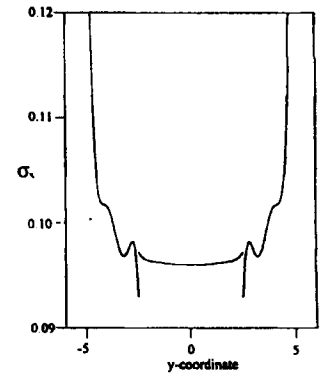

Mesh 3 (p=5)

Figure 11. Plot of the σ_{xx}-component of stress along the line $x = 10$ m for Problem 2

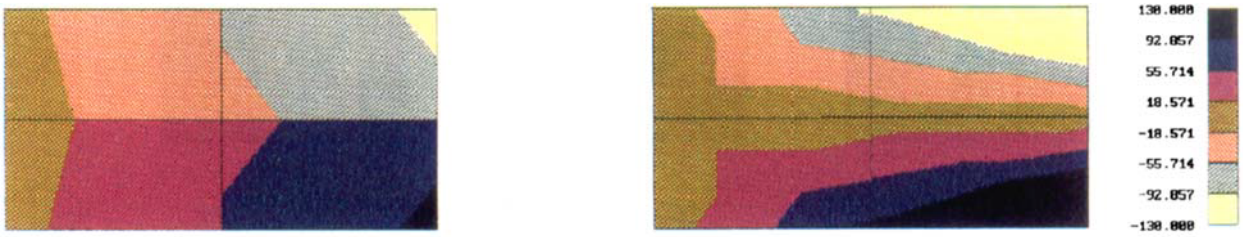

(a) (b)

Plate 1. Contours of the τ_{xy}-component of stress for Mesh 1 of Problem 1: (a) conforming (4-noded) element; (b) equilibrium (linear) element

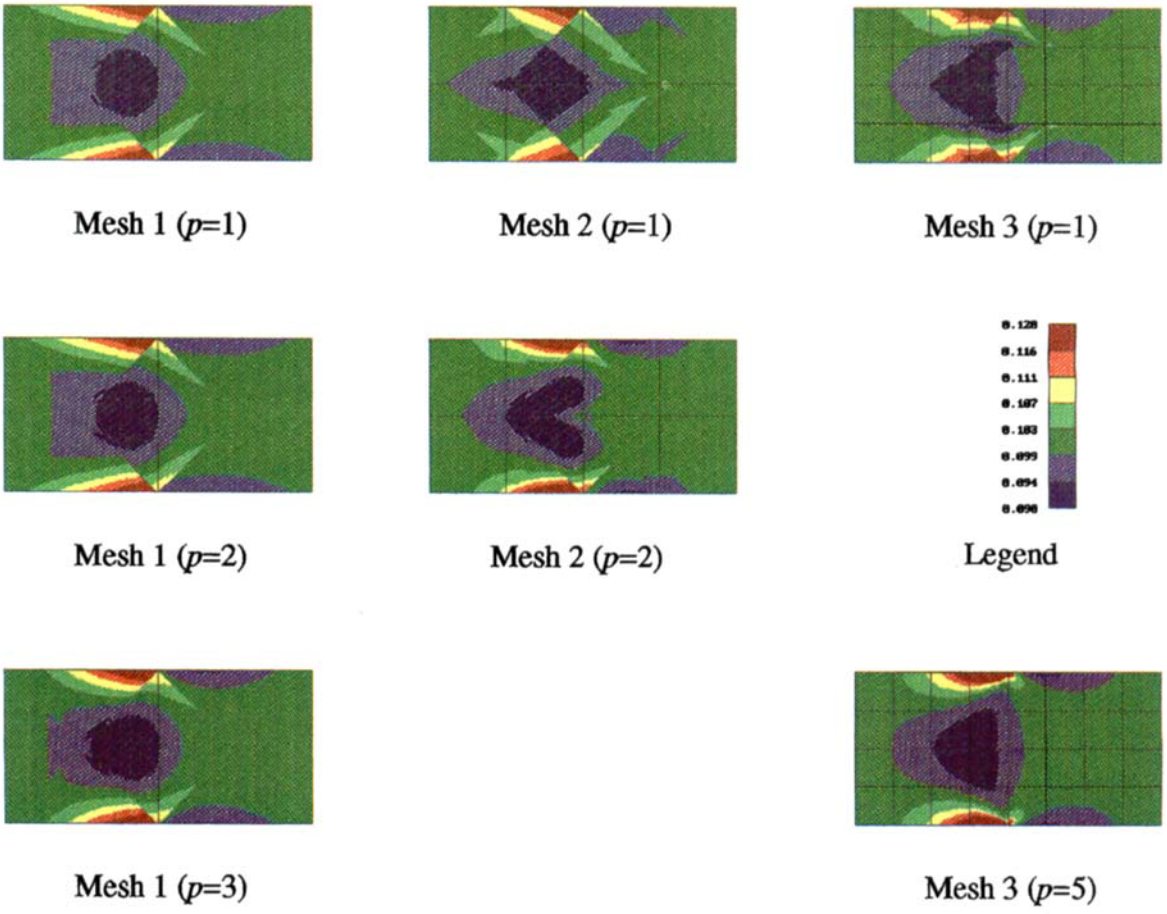

Plate 2. Contours of the σ_{xx}-component of stress for selected *p-h* combinations

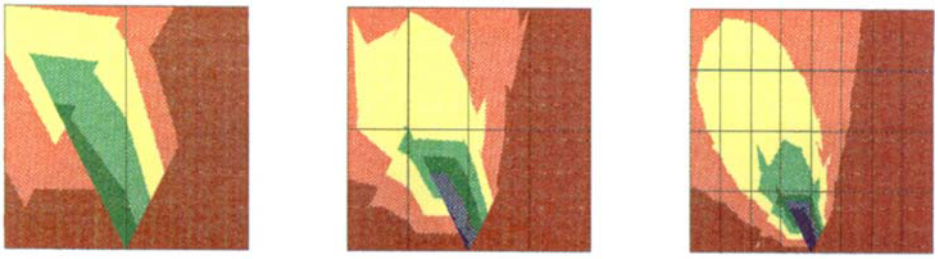

Mesh 1 (p=1) Mesh 2 (p=1) Mesh 3 (p=1)

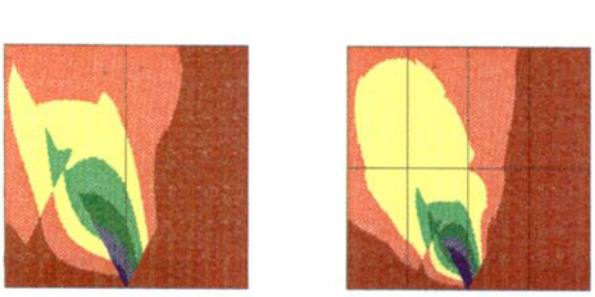

Mesh 1 (p=2) Mesh 2 (p=2) Legend

Mesh 1 (p=3) True solution

Plate 3. Convergence of the τ_{xy}-component of the stress for Problem 3

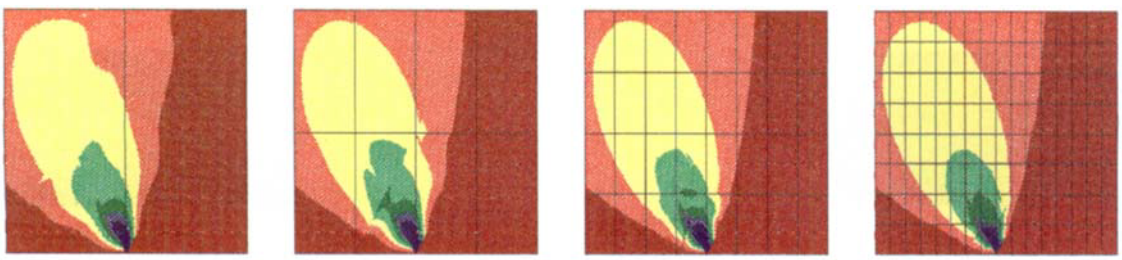

Mesh 1 p=5 dof=84 error=1.65%

Mesh 2 p=3 dof=176 error=1.73%

Mesh 3 p=2 dof=456 error=1.46%

Mesh 4 p=1 dof=1120 error=1.64%

Plate 4. Contours of the τ_{xy}-component of stress for similar errors in strain energy

Symmetric boundary conditions are applied on the line of symmetry. For Young's modulus $E = 210\,\mathrm{N/m^2}$, Poisson's ratio $\nu = 0{\cdot}3$, and a material thickness $t = 0.1$ m with a plane stress assumption, the strain energy U for the symmetric half shown is 62·442963 N m.[28].

The strain energy results from the finite element analyses performed on the four meshes shown in Figure 12(b) are given in Table V.

Figure 13 shows the convergence characteristics of the finite element strain energies. Note the significantly increased rate of convergence obtained with p-refinement compared with h-refinement. For Mesh 4, the 8-noded displacement element gives a finite element strain energy of ${}^{8}U_h^{C} = 61{\cdot}056022$ N m (866 dof) thereby confirming the bounded nature of the two types of solution.

The convergence of the stresses is demonstrated for the τ_{xy}-component of the stress in Plate 3, whilst that of the displacements is shown in Figure 14.

Although p-refinement has the faster convergence rate, it is of interest to consider qualitatively the stress fields obtained in the four meshes for the same energy of the error. For example, Plate 4

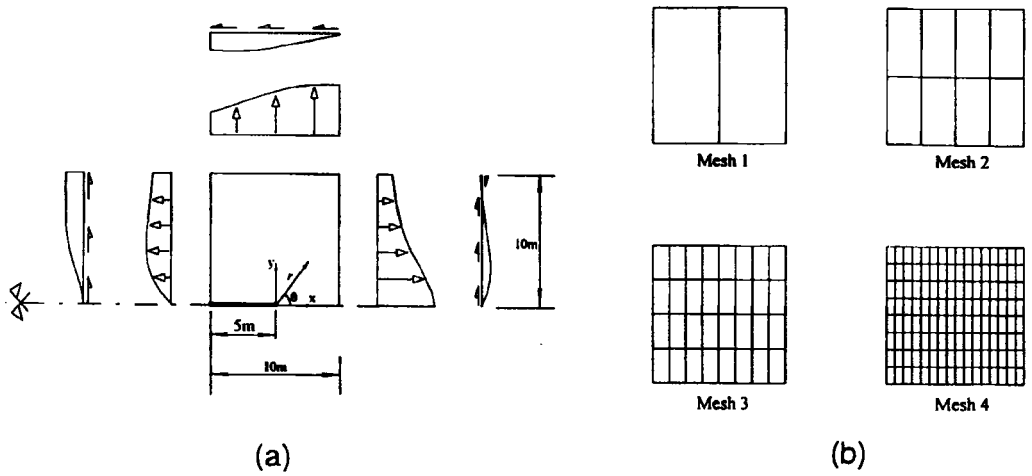

Figure 12. Problem 3: (a) the geometry and boundary conditions; (b) the meshes

Table V. Finite element results for Problem 3

	Mesh 1		Mesh 2		Mesh 3		Mesh 4	
p	U_h^E	dof	U_h^E	dof	U_h^E	dof	U_h^E	dof
1	73·313361	28	67·107610	88	64·577097	304	63·470253	1120
2	66·731729	42	64·333771	132	63·356702	456	62·892746	1680
3	64·713918	56	63·525367	176	62·974219	608	62·706200	2240
4	63·909238	70	63·153881	220	62·794140	760	62·617507	2800
5	63·471788	84	62·946635	264	62·692650	912	62·567278	3360
6	63·207607	98	62·819312	308	62·629937	1064	62·536154	3920
7	63·034270	112	62·735024	352	62·588271	1216	62·515438	4480
8	62·914096	126	62·676244	396	62·559142	1368	62·500936	5040
9	62·827305	140	62·633612	440	62·537979	1520	62·490399	5600
10	62·762547	154	62·601702	484	62·522117	1672	62·482472	6160

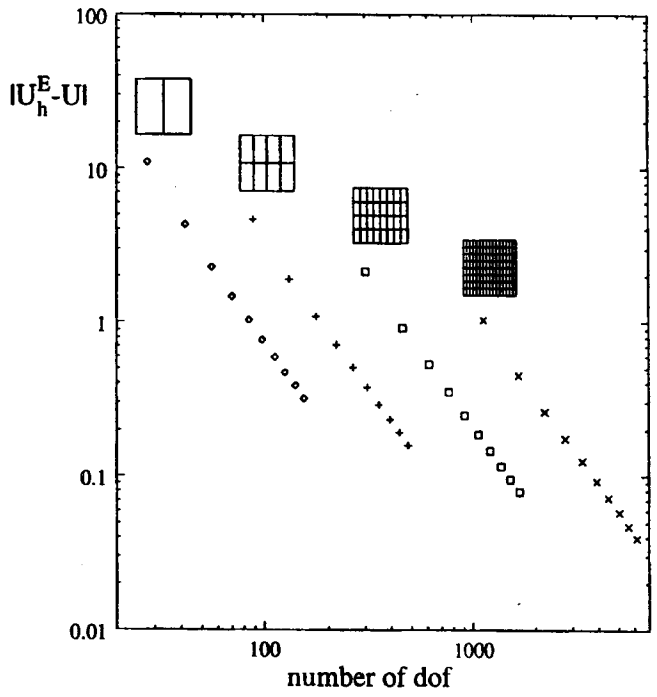

Figure 13. Convergence characteristics of the equilibrium models for Problem 3

shows τ_{xy} for the four meshes when the error is approximately 1·6 per cent in energy terms. This corresponds to $\log(U_h^E - U) \approx 0$ in Figure 13. It appears that the continuity and quality of τ_{xy} does improve with the number of degrees of freedom achieved with h-refinement.

9. CONCLUSIONS

1. By recognizing the general properties of macro-elements, a p-type equilibrium element has been formulated which effectively removes the usual problems associated with spurious kinematic modes.
2. Numerical examples with rectangular macro-elements with p in the range 1 to 10 confirm the feasibility of the proposed formulation, and indicate that solutions of good quality are obtainable for both statically admissible stress fields *and* side displacements.
3. Numerical examples indicate that, in energy terms, p-refinement produces much faster convergence than h-refinement. However, for the same overall error, it appears that the stress fields from p-refinement of a coarse mesh, although incurring less degrees of freedom, are inferior to those obtained with some h-refinement.
4. Further work is required to:

   (a) Formally prove the observed properties of the macro-elements as regards spurious kinematic modes.

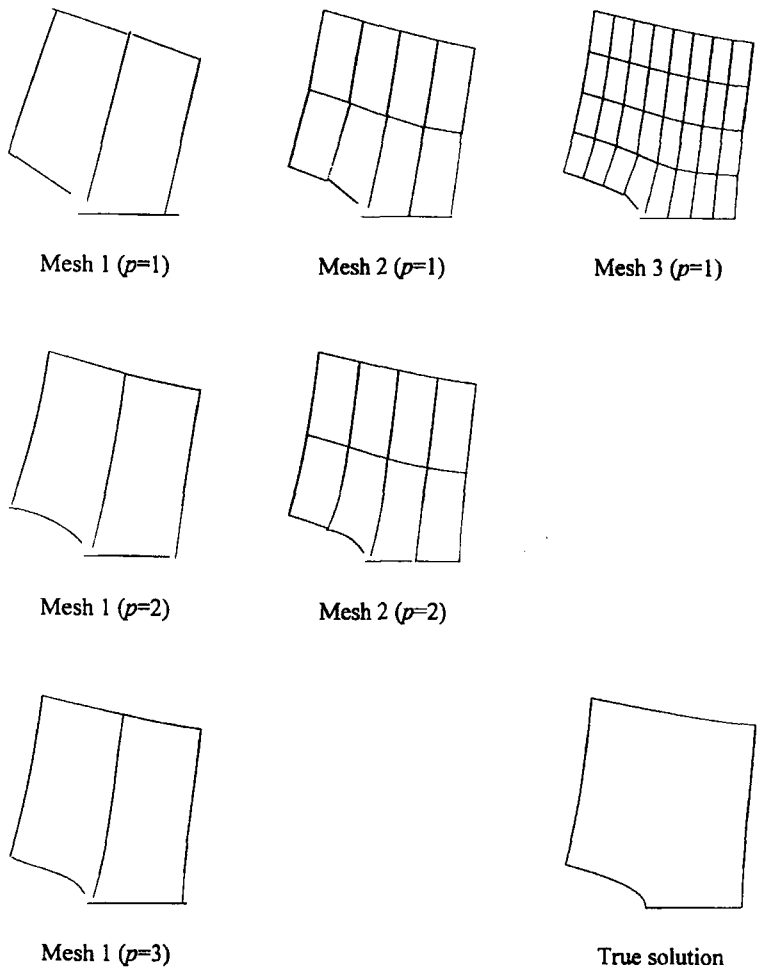

Figure 14. Convergence of the displaced shape for Problem 3

(b) Investigate alternative numerical procedures for the formulation of macro-elements, and their assembly into finite element equations, with a view to minimizing computational effort.
(c) Extend numerical studies to include triangular and general distorted quadrilateral macro-elements. These studies should also address such questions as: what are the optimum positions of the internal points P?
(d) Make a detailed comparison between equilibrium and displacement elements, both from the computational and the engineering points of view.

5. The p-refinement capability of the macro-element also makes it suitable for use in dual type error estimation of finite element models with hierarchical p-type displacement elements. This is in contrast to existing methods which approximate equilibrium solutions by using higher order displacement elements.[29,30]

REFERENCES

1. G. Sander, 'Application of the dual analysis principle', in B. Fraeijs de Veubeke (ed.), *High Speed Computing of Elastic Structures*, Vol. 61, Les Congres et Colloques de l'Universite de Liege, 1971, pp. 167–207.
2. B. Fraeijs de Veubeke, G. Sander and P. Beckers, 'Dual analysis by finite elements: linear and non linear applications', *Technical Report AFFDL-TR-72-93*, Ohio, 1972.
3. R. H. Gallagher, J. C. Heinrich and N. Sarigul, 'Complementary energy revisited', in S. N. Atluri, R. H. Gallagher and O. C. Zienkiewicz (eds.), *Hybrid and Mixed Finite Element Methods*, Chapter 23, Wiley, New York, 1983, pp. 453–465.
4. J. P. B. Moitinho de Almeida, 'Modelos de elementos finitos para a analise elastoplastica', Ph.D. thesis, Technical University of Lisbon, 1989.
5. T. H. H. Pian, 'Evolution of assumed stress hybrid finite elements', in J. Robinson (ed.), *ART in FEM Technology*, Robinson, Robinson and Associates, 1984, pp. 602–619.
6. J. Robinson, 'The mode-amplitude technique and hierarchical stress elements—a simplified and natural approach', *Int. j. numer. methods eng.*, **21**, 487–507 (1985).
7. J. Robinson, *Integrated Theory of Finite Element Methods*, Wiley, New York, 1973.
8. E. A. W. Maunder and G. J. Savage, 'A graph-theoretic model for finite elements with side variables', *Civil Eng. Syst.*, **11**, 111–141 (1994).
9. O. C. Zienkiewicz and R. Taylor, *The Finite Element Method*, 4th edn, McGraw-Hill, New York, 1989.
10. J. P. B. Moitinho de Almeida and J. A. Teixeira de Freitas, 'Alternative approach to the formulation of hybrid equilibrium finite elements', *Comput. Struct.*, **40**, 1043–1047 (1991).
11. A. C. A. Ramsay, 'Robust variable degree equilibrium elements: their formulation and application', Report for Human, Capital and Mobility Network, *ERB4050p1930382*, 1995.
12. M. Kieffer, 'Element de quadrilatere, statiquement admissible et co-diffusif, a champ de tensions du premier degre', *LTAS Report SF-5*, Universite de Liege, 1969.
13. M. Kieffer, 'Element quadrilateral de membrane, statiquement admissible et co-diffusif a champ des tensions du second degre', *LTAS Report SF-7*, Universite de Liege, 1970.
14. B. Fraeijs de Veubeke, 'Diffusive equilibrium models', in M. Geradin (ed.), *B. M. Fraeijs de Veubeke Memorial Volume of Selected Papers*, Sijthoff and Noordhoff/Waterloo University, 1980, pp. 569–628.
15. E. A. W. Maunder, 'A direct approach to a flexibility matrix for a triangular equilibrium membrane element', in J. Robinson (ed.), *Accuracy, Reliability and Training in FEM Technology*, Robinson and Associates, 1984, pp. 119–128.
16. D. J. Allman, 'The linear stress triangular equilibrium model in plane elasticity', *Comput. Struct.*, **31**, 673–680 (1989).
17. E. A. W. Maunder and W. G. Hill, 'Complementary use of displacement and equilibrium models in analysis and design', in J. Robinson (ed.,) *FEM in the Design Process*, Robinson and Associates, 1990, pp. 493–501.
18. E. A. W. Maunder and A. C. A. Ramsay, 'Quadratic equilibrium elements', in J. Robinson (ed.), *FEM Today and the Future*, Robinson and Associates, 1993, pp. 401–407.
19. V. B. Watwood and B. V. Hartz, 'An equilibrium stress field model for finite element solutions of two-dimensional elastostatic problems', *Int. J. Solids. Struct.*, **4**, 857–873 (1968).
20. C. Johnson and B. Mercier, 'Some equilibrium finite element methods for two-dimensional problems in continuum mechanics', in R. Glowinski, E. Y. Rodin and O. C. Zienkiewicz (eds.), *Energy Methods in Finite Element Analysis*, Chapter 11, Wiley, New York, 1979, pp. 213–224.
21. A. Zavelani-Rossi, 'Collapse load analysis by finite elements', in M. Z. Cohn and G. Maier (eds), *Engineering Plasticity by Mathematical Programming*, Chapter 11, Pergamon, New York, 1979, pp. 257–269.
22. P. Ladeveze, G. Coffignal and J. P. Pelle, 'Accuracy of elastoplastic and dynamic analysis', in I. Babuska, O. C. Zienkiewicz, J. Gago, E. R. de A. Oliveira (eds.), *Accuracy Estimates and Adaptive Refinements in Finite Element Computations*, Chapter 11, Wiley, New York, 1986, pp. 181–203.
23. P. Rougeot, 'Sur le controle de la qualite des maillages elements finis', Ph.D. Thesis, Universite Paris 6, 1989.
24. P. Temin-Gendron, and P. Laurent-Gengoux, 'Calculation of limit loads for composite materials via equilibrium finite elements', *Comput. Struct.*, **45**, 947–957 (1992).
25. E. A. W. Maunder, 'A reappraisal of compound equilibrium elements', in M. A. Erki and J. Kirkhope (eds.), *Proc. 12th Canadian Congress of Applied Mechanics*, Carleton University, 1989, pp. 796–797.
26. G. Strang, *Linear Algebra and its Applications*, 3rd edn, Harcourt Brace Jovanovich, 1988.
27. B. Szabo and I. Babuska, *Finite Element Analysis*, Wiley, New York, 1991.
28. A. C. A. Ramsay, 'Finite element shape sensitivity and error measures', *Ph.D. Thesis*, University of Exeter, 1994.
29. H. Ohtsubo and M. Kitamura, 'Element by element *a posteriori* estimation and improvement of stress solutions for two-dimensional elastic problems', *Int. j. numer. methods eng.*, **29**, 223–244 (1990).
30. M. Ainsworth, J. T. Oden, W. Wu, '*A posteriori* error estimation for *h–p* approximations in elastostatics', *Appl. Num. Math.*, **14**, 23–54 (1994).